Cellular/Molecular

Functional Role of GABAergic Innervation of the Cochlea: Phenotypic Analysis of Mice Lacking $GABA_A$ Receptor Subunits $\alpha1$, $\alpha2$, $\alpha5$, $\alpha6$, $\beta2$, $\beta3$, or δ

Stéphane F. Maison,[1] Thomas W. Rosahl,[2] Gregg E. Homanics,[3] and M. Charles Liberman[1]

[1]Department of Otology and Laryngology, Harvard Medical School and Eaton–Peabody Laboratory, Massachusetts Eye and Ear Infirmary, Boston, Massachusetts 02114, [2]Neuroscience Research Center, Merck Sharp and Dohme Research Laboratories, Harlow, Essex CM20 2QR, United Kingdom, and [3]Departments of Anesthesiology and Pharmacology, University of Pittsburgh, Pittsburgh, Pennsylvania 15260

The olivocochlear efferent system is both cholinergic and GABAergic and innervates sensory cells and sensory neurons of the inner ear. Cholinergic effects on cochlear sensory cells are well characterized, both *in vivo* and *in vitro*; however, the robust GABAergic innervation is poorly understood. To explore the functional roles of GABA in the inner ear, we characterized the cochlear phenotype of seven mouse lines with targeted deletion of a $GABA_A$ receptor subunit ($\alpha1$, $\alpha2$, $\alpha5$, $\alpha6$, $\beta2$, $\beta3$, or δ). Four of the lines ($\alpha1$, $\alpha2$, $\alpha6$, and δ) were normal: there was no cochlear histopathology, and cochlear responses suggested normal function of hair cells, afferent fibers, and efferent feedback. The other three lines ($\alpha5$, $\beta2$, and $\beta3$) showed threshold elevations indicative of outer hair cell dysfunction. $\alpha5$ and $\beta2$ lines also showed decreased effects of efferent bundle activation, associated with decreased density of efferent terminals on outer hair cells: although the onset of this degeneration was later in $\alpha5$ ($>$6 weeks) than $\beta2$ ($<$6 weeks), both lines shows normal efferent development (up to 3 weeks). Two lines ($\beta2$ and $\beta3$) showed signs of neuropathy, either decreased density of afferent innervation ($\beta3$) or decreased neural responses without concomitant attenuation of hair cell responses ($\beta2$). One of the lines ($\beta2$) showed a clear sexual dimorphism in cochlear phenotype. Results suggest that the GABAergic component of the olivocochlear system contributes to the long-term maintenance of hair cells and neurons in the inner ear.

Key words: **efferent; hair cell; olivocochlear; auditory; feedback; knock-out mice**

Introduction

The mammalian cochlea is innervated by a feedback efferent pathway, the olivocochlear (OC) bundle, consisting of two subsystems (supplemental Fig. S1, available at www.jneurosci.org as supplemental material): a medial component projecting to electromotile outer hair cells (OHCs) and a lateral component innervating auditory-nerve dendrites, close to their synapses with inner hair cells (IHCs) (Warr and Guinan, 1979). OHC efferents, when activated, raise cochlear thresholds by decreasing OHC contributions to cochlear mechanical amplification (Guinan, 1996). This fast feedback inhibition is a cholinergic effect, mediated by $\alpha9/\alpha10$ acetylcholine (ACh) receptors (Vetter et al., 1999). The efferent projections to afferent dendrites can elicit either slow excitation or inhibition of the cochlear nerve, suggesting two functional subgroups (Groff and Liberman, 2003). However, the transmitter(s) and receptor(s) involved in these lateral OC effects are not clear.

Both medial and lateral efferents contain GABA (Fex and Altschuler, 1986; Eybalin, 1993), and cholinergic and GABAergic markers colocalize in most efferent terminals (Maison et al., 2003a). Immunostaining for $GABA_A$ receptors has been reported on cochlear nerve somata, OHCs, and in the region of synaptic contact between lateral OC terminals and cochlear nerve afferents (Plinkert et al., 1989, 1993; Yamamoto et al., 2002). Reverse transcription (RT)-PCR and *in situ* hybridization suggest cochlear expression of most $GABA_A$ receptor subunits (Drescher et al., 1993; Kempf et al., 1994, 1995).

Despite evidence for a robust GABAergic network, there is little agreement as to its functional role. Some *in vitro* studies report that GABA elicits OHC hyperpolarization and changes in motility (Gitter and Zenner, 1992; Batta et al., 2004), whereas others report no effects (Dulon et al., 1990; Evans et al., 1996). In frog lateral line, GABA suppresses spontaneous afferent discharge (Mroz and Sewell, 1989); however, in guinea pig, GABA has no effect on spontaneous activity (Arnold et al., 1998). Cochlear perfusion of GABA antagonists blocked slow amplitude fluctuations of an otoacoustic emission (Kirk and Johnstone, 1993); however, these fluctuations persisted after complete neural blockade (Kujawa et al., 1995).

The present study probes the functional role of cochlear

Received Sept. 13, 2005; revised Aug. 25, 2006; accepted Aug. 29, 2006.

This work was supported by National Heart Institute–National Institute on Deafness and Other Communication Disorders Grants RO1 DC 00188 and P30 DC 005029. We thank Dr. W. Wisden (University of Heidelberg, Heidelberg, Germany) for providing $\alpha6$ $GABA_A$ knock-outs and Dr. J. J. Guinan Jr and W. F. Sewell for comments on this manuscript. The skillful assistance of Leslie Dodds and Constance Miller is gratefully acknowledged.

Correspondence should be addressed to Dr. Stéphane F. Maison, Eaton–Peabody Laboratory, Massachusetts Eye and Ear Infirmary, 243 Charles Street, Boston, MA 02114-3096. E-mail: stephane_maison@meei.harvard.edu.

DOI:10.1523/JNEUROSCI.2395-06.2006

 0270-6474/06/2610315-12$15.00/0

Table 1. Numbers of mice examined from each genotype, from each line, for each of the physiological and histological analyses performed in the present study

	α1	α2	α5				α6	β2				β3		δ
	6 weeks	6 weeks	1.5 weeks	3 weeks	6 weeks	24 weeks	6 weeks	1.5 weeks	3 weeks	6 weeks	24 weeks	6 weeks	24 weeks	6 weeks
Thresholds (ABR)	+/+ 4	+/+ 10			+/+ 15	+/+ 12				+/+ 17	+/+ 13	+/+ 8		+/+ 13
	−/− 7	−/− 8			−/− 8	−/− 10	−/− 7			−/−22	−/− 22	+/− 11		−/− 11
												−/− 17		
Thresholds (DPOAE)	+/+ 9	+/+ 17			+/+ 29	+/+ 23				+/+ 33	+/+ 23	+/+ 16		+/+ 26
	−/− 13	−/− 16			−/− 35	−/− 20	−/− 14			−/− 48	−/− 29	+/− 22		−/− 22
												−/− 17		
Efferent function	+/+ 12	+/+ 4			+/+ 11					+/+ 6				+/+ 8
	−/− 10	−/− 6			−/− 9					−/− 17				−/− 5
Cochlear vulnerability					+/+ 5					+/+ 6				
					−/− 6					−/− 9				
Cochlear pathology	+/+ 2	+/+ 2			+/+ 2	**				+/+ 4	+/+ 2	+/+ 2		+/+ 2
	−/− 2	−/− 2			−/− 2	−/− 3	−/− 2			−/− 5	−/− 2	−/− 3	−/− 2	−/− 2
Cochlear innervation			+/+ 2	+/+ 1	+/+ 1	+/+ 1		**	+/+ 1	+/+ 2			+/+ 1	
			−/− 2	−/− 2	−/− 1	−/− 3		−/− 2	−/− 2	−/− 3			−/− 2	

**, Data from genetically identical β2 or α5 +/+ ears were used. All animals examined for histopathology were also tested by ABR and DPOAE. Results of ABR and DPOAE tests are shown in Figures 1 and 2 and supplemental Figure S1 (available at www.jneurosci.org as supplemental material). Results of the assay for efferent function are shown in Figure 3 and supplemental Figure S2 (available at www.jneurosci.org as supplemental material), for cochlear vulnerability in Figure 4, for cochlear histopathology in Figures 5 and 6, and for cochlear innervation in Figures 7–9.

GABAergic transmission by assessing (1) cochlear function, (2) effects of efferent activation, (3) vulnerability to acoustic injury, (4) cochlear histopathology, and (5) cochlear innervation in seven mouse lines, each with a different $GABA_A$ receptor subunit targeted for deletion: α1, α2, α5, α6, β2, β3, or δ. $GABA_A$ receptors are ligand-gated chloride channels consisting of a pentameric assembly of subunits. To date, 19 subunit-encoding genes have been cloned, including α1–α6, β1–β3, γ1–γ3, and δ (Whiting, 1999). Most receptors *in vivo* combine two α and two β subunits with either a γ or δ subunit (Vicini and Ortinski, 2004).

Our data show dramatic auditory effects in three mutant lines (α5, β2, and β3), and thereby provide unequivocal evidence for *in vivo* functional role(s) of the GABAergic innervation of the cochlea. The nonauditory phenotypes of $GABA_A$ mutants are subtle, suggesting compensation by subunit substitution and/or plasticity in other elements of the neuronal circuitry underlying the high-level behaviors assayed (e.g., spatial learning, locomotor activity, etc.). In contrast, the dramatic cochlear phenotypes may reflect the comparative simplicity of inner ear circuitry.

Materials and Methods

Experimental procedures. Seven knock-out mouse lines, each lacking one of the $GABA_A$ receptor subunits, were studied for the present report. Most lines are healthy, fertile, and display only subtle behavioral phenotypes [α1 (Sur et al., 2001); α2 (Boehm et al., 2004); α5 (Collinson et al., 2002); α6 (Jones et al., 1997); β2 (Sur et al., 2001); δ (Mihalek et al., 1999)]. Only the β3 knock-outs have an overt phenotype: 90% die within 24 h of birth; those that survive are runts at weaning, hyperactive, and show poor motor coordination and poor performance on learning and memory (Homanics et al., 1997; DeLorey et al., 1998; Vicini and Ortinski, 2004). Experimental design for this line was severely constrained by the rarity and fragility of the animals.

Techniques used for the creation of each mutant line, the genotyping, and the characterization of nonauditory phenotypes are described in previous publications: α1 (Vicini et al., 2001), α2 (Boehm et al., 2004), α5 (Collinson et al., 2002), α6 (Jones et al., 1997), β2 (Sur et al., 2001), β3 (Homanics et al., 1997), and δ (Mihalek et al., 1999). All mutant lines represent hybrids of 129 strains (stem cell donor) and C57BL/6 (maternal strain). Because both "parental" strains can show early-onset age-related cochlear degeneration (Jimenez et al., 1999; Q. Y. Zheng et al., 1999), all testing was performed with age-matched wild-type littermates (generated from heterozygous matings) as controls. For six of the lines, breeding pairs of heterozygous animals were shipped from the laboratories of origin to the Massachusetts Eye and Ear Infirmary, where on-site breeding produced wild-type littermates and homozygous and heterozygous nulls for the present study of cochlear function and histopathology. For the $GABA_A$ α6 mutant line, only homozygous mutants were available; thus, no precisely appropriate wild-type animals were available. For all mutant lines, cochlear function was tested first at 6–8 weeks of age. In some lines, animals at older ages (~24 weeks) were also tested. All electrophysiological experiments were conducted in a temperature-controlled soundproof chamber maintained at ~32°C. The care and use of the animals reported in this study was approved by the Institutional Animal Care and Use Committee of the Massachusetts Eye and Ear Infirmary. Numbers of animals of each strain/genotype subjected to the various functional and histological tests are listed in Table 1.

Auditory brainstem responses. Mice were anesthetized with xylazine (20 mg/kg, i.p.) and ketamine (100 mg/kg, i.p.). Needle electrodes were inserted at vertex and pinna, with a ground near the tail. Auditory brainstem responses (ABRs) were evoked with 5 ms tone pips (0.5 ms rise-fall, $\cos^2$ onset, at 35/s; acoustic system is described below). The response was amplified (10,000×), filtered (100 Hz to 3 kHz), and averaged with an analog-to-digital board in a LabVIEW (National Instruments, Austin, TX)-driven data-acquisition system. Sound level was raised in 5 dB steps from 10 dB below threshold to 80 dB sound pressure level (SPL). At each level, 1024 responses were averaged (with stimulus polarity alternated), using an "artifact reject" whereby response waveforms were discarded when peak-to-peak amplitude exceeded 15 μV. During visual inspection of stacked waveforms, "threshold" was defined as the lowest SPL level at which any wave could be detected, usually the level step just below that at which the response amplitude exceeded the noise floor (~0.25 μV). For amplitude versus level functions, wave I peak was identified by visual inspection at each sound level, and the peak-to-peak amplitude was computed.

Distortion product otoacoustic emissions. Mice were anesthetized as for ABR measures. Distortion product otoacoustic emissions (DPOAEs) at $2f_1 - f_2$ were recorded with a custom acoustic assembly consisting of two electrostatic drivers (TDT EC-1; Tucker-Davis Technologies, Alachua, FL) to generate primary tones (f_1 and f_2 with $f_2/f_1 = 1.2$ and f_2 level 10 dB $< f_1$ level) and a Knowles (Itasca, IL) miniature microphone (EK3103) to record ear-canal sound pressure. Stimuli were generated digitally, whereas resultant ear-canal sound pressure was amplified and digitally sampled at 4 μs (16 bit data acquisition DAQ boards, NI 6052E; National Instruments). Fast Fourier transforms were computed and averaged over five consecutive waveform traces, and $2f_1 - f_2$ DPOAE amplitude and surrounding noise floor were extracted, a procedure requiring ~4 s of data acquisition and processing time. Iso-responses were interpolated from plots of amplitude versus sound level, performed in 5 dB steps of f_1 level. Threshold is defined as the f_1 level required to produce a DPOAE with amplitude of 0 dB SPL.

Medial olivocochlear assay. Mice were anesthetized with urethane (1.20

g/kg, i.p.). A posterior craniotomy and partial cerebellar aspiration were performed to expose the floor of the IVth ventricle. To stimulate the OC bundle, shocks (monophasic pulses, 150 μs duration, 200/s) were applied through fine silver wires (0.4 mm spacing) placed along the midline, spanning the OC decussation. Shock threshold for facial twitches was determined, muscle paralysis was induced with α-D-tubocurarine (1.25 mg/kg, i.p.), and the animal was connected to a respirator via a tracheal cannula. Shock levels were raised to 6 dB above twitch threshold. During the OC suppression assay, f_2 level was set to produce a DPOAE 10–15 dB > noise floor. To measure OC effects, repeated measures of baseline DPOAE amplitude were first obtained ($n = 12$), followed by a series of 17 contiguous periods in which DPOAE amplitudes were measured with simultaneous shocks to the OC bundle and 30 additional periods during which DPOAE measures continued after the termination of the shock train. The magnitude of the efferent effect is defined as the suppression of DPOAE amplitude, i.e., the decibel difference between the mean of the first three during-shock points and the mean of the 12 pre-shock measures. In data from normal ears, the magnitude of shock-evoked efferent effects diminishes as cochlear thresholds increase (Guinan and Gifford, 1988). Thus, when wild-type animals in the present study showed lower cochlear thresholds than their littermate mutants, we adjusted (reduced) the efferent effect magnitudes measured in wild types according to a linear regression between threshold and efferent effect size obtained for a large database of 108 wild-type (control) mice from 17 mutant strains (Maison and Liberman, 2006).

Acoustic overexposure. Animals were exposed, awake and unrestrained, within cages suspended inside a small reverberant sound-exposure box (Liberman and Gao, 1995). The exposure stimulus was generated by a custom-made white-noise source, filtered (Brickwall Filter with a 60 dB/octave slope), amplified [Crown (Elkhart, IN) power amplifier], and delivered [JBL (Northridge, CA) compression driver] through an exponential horn fitted to the top of a reverberant box. Sound pressure was calibrated daily by positioning the one-quarter-inch condenser microphone at the approximate position of the animal's head. Acoustic trauma consisted of a 2 h exposure to an 8–16 kHz band noise presented at 89 dB SPL.

Cochlear processing and immunostaining. After a terminal experiment, matched sets of wild-type and mutant mice were perfused intracardially for histological assessment via either plastic sections of osmium-stained cochleae or organ of Corti whole mounts immunostained for neurofilament (NF) and/or vesicular acetylcholine transporter (VAT) to label the afferent and efferent innervation. For plastic-embedded, sectioned material, intravascular fixative was 2.5% glutaraldehyde and 1.5% paraformaldehyde in phosphate buffer. Cochleae were decalcified in EDTA, osmicated and dehydrated in ethanols and propylene oxide, embedded in Araldite resins, and sectioned at 40 μm on a Historange with a carbide steel knife. Sections were mounted on slides and coverslipped. For cochlear whole mounts, intravascular fixation was with 4% paraformaldehyde plus 0.1% glutaraldehyde in PBS. Cochleas were decalcified, dissected into half-turns, and then incubated in 5% normal horse serum with 0.03% Triton X-100 in PBS for 1 h. This was followed by incubation in primary antibody(s) [mouse anti-200 kDa-NF from MP Biomedicals (Irvine, CA) at 1:50,000 and/or rabbit anti-VAT from Sigma (St. Louis, MO) at 1:1000] for ~19 h, followed by secondary antibody (biotinylated donkey anti-mouse (Jackson ImmunoResearch, West Grove, PA) and/or Alexa Fluor-488 chicken anti-rabbit (Invitrogen, Carlsbad, CA)] for 90 min. In early experiments with anti-NF staining, an avidin–biotin–HRP complex linkage (ABC kit; Vector Laboratories, Burlingame, CA) and DAB/H_2O_2 chromogen reaction, with a silver enhancement step, were used. In later experiments, double-stained material, streptavidin-coupled Alexa Fluor-568 was bound to the biotinylated donkey anti-mouse secondary antibody.

To immunolocalize the $GABA_A$ receptors in cochlear tissue, cochleas from wild-type and mutant animals were harvested after intravascular perfusion with 4% paraformaldehyde plus 0.1% glutaraldehyde in PBS, postfixed from 2 to 18 h, rinsed, and decalcified in EDTA. After cryoprotection and infiltration of OCT, frozen sections were cut at 14 μm and mounted on slides. The following primary antibodies were used in experiments to localize the $GABA_A$ receptors: α1 (rabbit) and β2/3 (mouse) from Upstate Biotechnologies (Charlottesville, VA); and α5 (rabbit), β2 (rabbit), and β3 (rabbit) from Novus Biologicals (Littleton, CO). The best results were obtained in material in which the biotinylated secondary antibody was followed by streptavidin-coupled Alexa Fluor-568.

Immunostaining analysis of cochlear innervation. The single-stained material (anti-neurofilament antibody) with DAB reaction product was wet mounted in Vectashield (Vector Laboratories) and placed on glass slides for examination in the light microscope via Nomarski optics with a 100× oil-immersion lens. In selected regions, focal z-series (0.5 μm step size) were obtained using MetaMorph software (Molecular Devices, Sunnyvale, CA) controlling a stepping motor on the fine focus. In double-staining experiments (anti-neurofilament and anti-VAT), tissue was mounted in Vectashield, coverslipped, and examined in a Leica (Nussloch, Germany) confocal microscope. In selected regions, focal z-series were obtained using 0.25 μm step size. For both kinds of image stacks, image projections in alternate planes were computed using Amira three-dimensional visualization software (Zuse Institute Berlin, Berlin, Germany). Amira was also used to compute the volume of immunostained OC terminals from the image stacks.

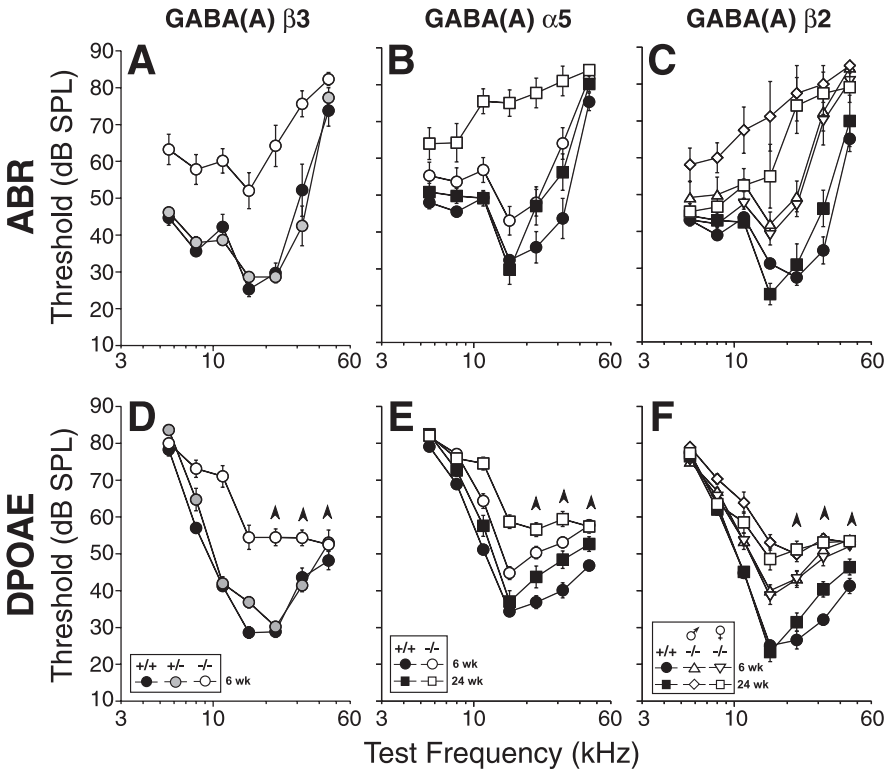

Figure 1. Three $GABA_A$ mutant lines, α5, β2, and β3, showed cochlear dysfunction when measured at 6 weeks; in both α5 and β2 lines, threshold shifts in ABR (***A–C***) and DPOAE (***D–F***) were even greater at 24 weeks. Group mean ± SEM thresholds for homozygous nulls (open symbols) are compared in each panel with wild-type littermates (filled symbols). Other aspects of symbology are explained in the keys. Upward arrowheads associated with DPOAE threshold more than ~60 dB indicate that, at these high frequencies, thresholds have reached stimulus levels producing passive distortion in the acoustic system and thus represent underestimates of true cochlear dysfunction.

Analysis of brainstem sections. Wild-type and homozygous null mice from the $\alpha 5$ and $\beta 2$ lines, aged 15–18 weeks, were perfused with 4% paraformaldehyde, and brainstems were extracted, postfixed overnight, cryoprotected in sucrose, and sectioned on a freezing microtome at 40 μm in the transverse plane. Serial sections spanning the olivary complex were treated histochemically to stain for acetylcholinesterase, which reveals the cell bodies of the olivocochlear neurons, using techniques described previously (Osen and Roth, 1969).

Histopathologic analysis of cochlear sections. All structures of the cochlear duct were analyzed in the entire set of serial plastic sections through each cochlea, and their conditions were noted in a spreadsheet according to a semiquantitative rating scale described previously (Wang et al., 2002). The condition of each structure as a function of cochlear frequency was then determined by (1) estimating the location of each section through the cochlear duct (in micrometers from the basal end) using average values extracted from true three-dimensional reconstructions of cochlear spirals from similarly embedded mouse cochleas (Wang et al., 2002) and (2) converting cochlear location to frequency according to a recently derived map for the mouse (Muller et al., 2005). The numbers of cochleas examined for each genotype and each mutant line are shown in Table 1.

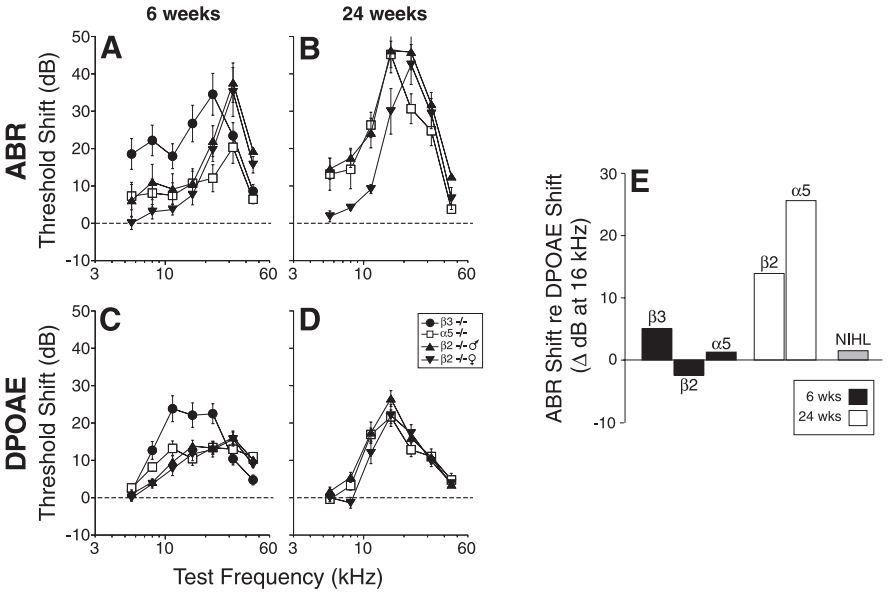

Figure 2. Mean cochlear thresholds in the three $GABA_A$ mutant lines with cochlear phenotype (data from Fig. 1) are replotted as threshold shifts by subtracting values obtained in knock-outs from mean values in wild types. ***A*** and ***B*** show ABR data for 6 and 24 weeks, respectively; ***C*** and ***D*** show DPOAE data for 6 and 24 weeks, respectively. In ***E***, comparison of ABR shifts and DPOAE shifts in these three lines suggests that the ongoing degeneration in $\beta 2$ and $\alpha 5$ lines is a type of neuropathy, i.e., ABR shifts $\gg$ DPOAE shifts. Data in ***E*** are shown only for the 16 kHz test frequency: each bar height in this panel is computed by subtracting the ABR shift (***A***, ***B***) from the DPOAE shift (***C***, ***D***) for the same mutant at the same group age. The bar labeled NIHL (noise-induced hearing loss) represents the difference between the mean ABR and DPOAE shifts at 16 kHz measured in a large group of CBA/CaJ mice after a noise exposure causing permanent cochlear damage that targets the OHCs (Wang et al., 2002) (S. G. Kujawa and M. C. Liberman, unpublished data).

Results

Cochlear thresholds

Assessment of baseline cochlear function was based on ABRs and DPOAEs. ABRs are averaged bioelectric potentials representing synchronous neural activity generated at several levels of the ascending auditory pathway. Cochlear nerve fibers contribute to the earliest wave, namely wave 1 (Melcher et al., 1996). DPOAEs arise as electrical distortions in electromechanical transduction, within the inner ear, that are reverse transduced into mechanical signals, amplified by OHCs, and then propagated back to the ear canal in which they can be measured in the sound pressure waveform (Lukashkin et al., 2002). Normal DPOAEs can be generated in the absence of inner hair cells or cochlear afferents (Liberman et al., 1997), whereas normal ABRs require normal function in all structures of the auditory periphery. Thus, measuring both ABRs and DPOAEs allows differential diagnosis in the sense that disparities can suggest the presence of auditory neuropathies (i.e., ABR shifts > DPOAE shifts).

In four of the mutant lines, $\alpha 1$, $\alpha 2$, $\alpha 6$, and δ, when tested at 6 weeks of age, there were no signs of cochlear threshold elevation (supplemental Fig. S2, available at www.jneurosci.org as supplemental material): mean thresholds for nulls and wild types were similar by both ABR and DPOAE tests. Although only homozygous nulls were available for the $\alpha 6$ line, thresholds are very similar to those in the other wild-type strains.

In the other three mutant lines, $\alpha 5$, $\beta 2$, and $\beta 3$, there was significant cochlear dysfunction (Fig. 1). At 6 weeks of age, the most severely affected mutants were those lacking the $\beta 3$ subunit. Mean ABR thresholds in $\beta 3$ nulls were elevated compared with wild types by 20–45 dB across test frequencies, with peak loss occurring at 22.6 kHz: Figure 1*A* shows absolute thresholds, and Figure 2*A* shows threshold differences between wild type and mutants.[a] This threshold elevation, corresponding to more than two orders of magnitude of stimulus amplitude, was highly significant (two-way ANOVA, $F_{(1,22)} = 19.982$; $p < 0.001$). Suprathreshold ABR amplitudes in $\beta 3$ nulls were significantly reduced in amplitude, by at least 50% at all frequencies and sound levels (data not shown). DPOAE thresholds were also significantly elevated across all test frequencies in $\beta 3$ nulls (Figs. 1*D*, 2*C*) (two-way ANOVA, $F_{(1,31)} = 50.193$; $p < 0.001$). In the middle of the cochlea (16 kHz), ABR shifts were similar in magnitude to the DPOAE shifts (Fig. 2*E*), suggesting that dysfunction in OHCs, or other processes involved in their role as cochlear amplifier, may account for the phenotype. Animals heterozygous for the $\beta 3$ deletion showed no threshold elevation (Fig. 1*A*).

At 6 weeks, $\alpha 5$ nulls and $\beta 2$ nulls showed similar patterns of threshold elevation (Figs. 1*B*,*C*, 2*A*): ABR data from both lines showed threshold shifts increasing from <5 to 20–30 dB with increasing tone frequency. Amplitudes of ABR suprathreshold responses (wave 1) were 25–50% lower in mutants compared with wild types, even at the highest stimulus levels (data not shown). DPOAE data also showed increasing threshold shifts from low to high frequencies (Fig. 2*C*). For both lines, these genotypic differences were highly significant by two-way ANOVA for both ABRs and DPOAEs: for $\alpha 5$ ABRs, $F_{(1,31)} = 9.674$, $p = 0.004$; for $\alpha 5$ DPOAEs, $F_{(1,62)} = 29.449$, $p < 0.001$; for $\beta 2$ ABRs, $F_{(1,37)} = 40.311$, $p < 0.001$; and for $\beta 2$ DPOAEs,

[a] In interpreting ABR or DPOAE measures, the dynamic ranges of the tests must be considered. For ABR measure, wild-type thresholds in all lines at the highest test frequency were close to 80 dB SPL, the highest sound pressure levels routinely presented. Thus, it would be impossible to register a significant shift at this frequency, and measured ABR shifts are underestimates at 45 kHz. The same holds for the DPOAE test, for the lowest test frequency presented (5.6 kHz). The DPOAE test has the additional limitation that the acoustic system begins to distort at input levels >60 dB SPL for 32 and 45 kHz. In summary, the most reliable frequency for quantitatively comparing ABR and DPOAE shifts is 16 kHz.

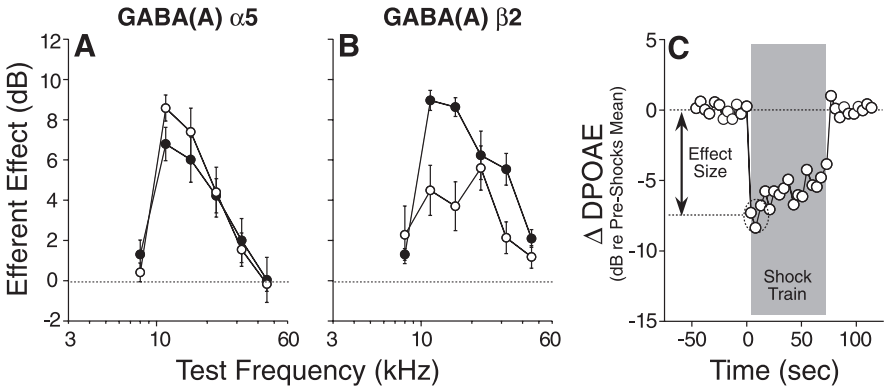

Figure 3. OHC efferent function is diminished in $GABA_A$ $\beta 2$ mutants and unaffected in $\alpha 5$ [and 3 other lines tested (supplemental Fig. S3, available at www.jneurosci.org as supplemental material). Efferent function was assessed by measuring DPOAE suppression caused by efferent-bundle shocks, normalized as described in Materials and Methods. ***A***, ***B***, Group mean ± SEM data for suppression magnitude for each of the six test frequencies in the mutant indicated. Numbers of animals tested in each genotype from each strain are in Table 1. ***C*** shows typical data from one run of this assay: DPOAE amplitude was measured 12 times during a ~70 s period, after which the shock train was turned on. The magnitude of the efferent effect is defined in Materials and Methods.

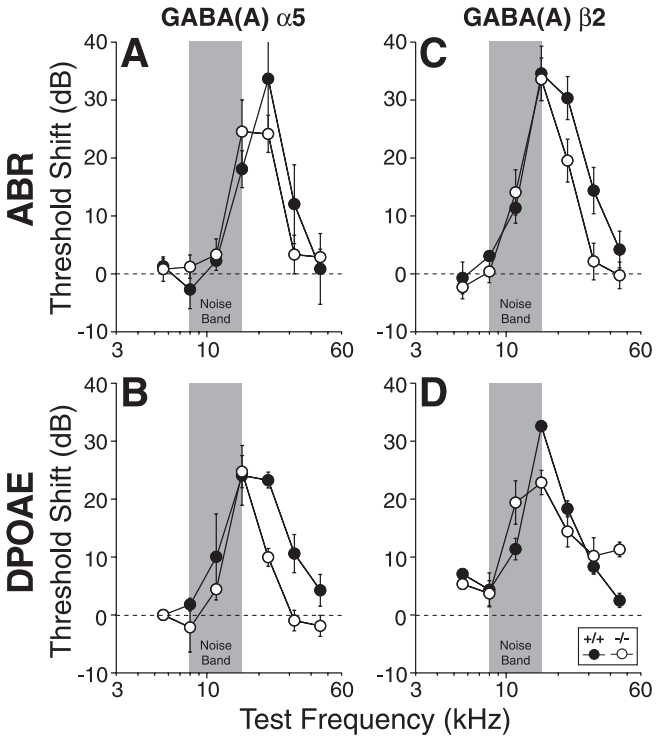

Figure 4. Exposure to high-level noise designed to cause severe, but reversible, threshold shifts does not reveal any differences in cochlear vulnerability attributable to loss of either the $\alpha 5$ or $\beta 2$ subunits. Group mean ± SEM threshold shifts are shown for ABR and DPOAE measured 12 h after exposure to a 8–16 kHz noise band at 89 dB SPL for 2 h. Threshold shift is defined as the difference between preexposure and postexposure values for the same groups of animals. Group sizes can be extracted from the row labeled "Cochlear vulnerability" in Table 1.

$F_{(1,73)} = 66.273$, $p < 0.001$. As seen in $\beta 3$ mutants, the magnitude of DPOAE shifts and ABR shifts were comparable (Fig. 2*E*), again suggesting that the threshold shift arises at, or before, the stage of OHC transduction and amplification.

When retested at 24 weeks, both $\alpha 5$ and $\beta 2$ null mice showed increased cochlear dysfunction compared with wild-type littermates: mean ABR threshold shifts in $\alpha 5$ and $\beta 2$ nulls peaked at 45 dB for test frequencies in the middle of the cochlea (Figs. 1*B*,*C*, 2*A*,*B*). Furthermore, a sexual dimorphism was revealed in the $\beta 2$ line, with males showing significantly more threshold shift than females (Figs. 1*C*, 2*B*). The sex differences were statistically significant at 24 weeks (two-way ANOVA, $F_{(1,8)} = 7.103$; $p = 0.029$) but not at 6 weeks. Although the gender differences appear greater at low than high frequencies, the 80 dB limit on test tone sound level may reduce the measurable elevations at high frequencies in the males. Sex differences were not significant for any of the other lines at any age tested.

ABR shifts were significantly larger than the DPOAE shifts for both the $\alpha 5$ and $\beta 2$ nulls at the 24 week test age (Fig. 2*E*). This disparity suggests that much of the progressive dysfunction is attributable to changes in the cochlear afferents or the inner hair cells that drive them, consistent with the robust GABAergic innervation of the inner hair cell area in the mouse (Maison et al., 2003a).

Efferent function

Activation of the efferent fibers terminating on OHCs elevates cochlear thresholds by decreasing OHC contributions to cochlear amplification (Guinan, 1996). This efferent effect is dominated by effects of ACh released by efferent terminals acting on the $\alpha 9/\alpha 10$ complex of nicotinic ACh receptors on OHCs (Vetter et al., 1999). Given published reports of GABAergic effects on length and stiffness of isolated OHCs (Plinkert et al., 1993; Batta et al., 2004) and given the reported colocalization of GABAergic and cholinergic markers in efferent terminals on OHCs (Maison et al., 2003a), we wondered whether loss of $GABA_A$ receptor subunits might affect the magnitude or time course of efferent-mediated cochlear suppression.

To assay efferent effects, DPOAE magnitudes were measured repeatedly, before, during, and after a 70 s train of shocks to the efferent bundle. In the example in Figure 3*C*, DPOAEs evoked with f_2 at 16 kHz were initially reduced by ~7 dB after the shock train was turned on. As the shock train continued, the suppression declined toward a steady state, which was maintained throughout the shock epoch, and the DPOAE returned to preshock baseline after the shocks were turned off. To assess the strength of efferent effects along the cochlear spiral, the test tones used to evoke the DPOAEs were varied from 5.6 to 45.2 kHz in half-octave steps. For wild-type animals from all five lines studied, the average suppression strength was greatest for test tones in the middle of that range (11–22 kHz) (Fig. 3*A*,*B*) (supplemental Fig. 3, available at www.jneurosci.org as supplemental material), in which DPOAEs are typically suppressed by 8–10 dB. This pattern has been seen in all mouse strains investigated (Vetter et al. 1999; Maison et al., 2002, 2003b) and reflects the corresponding apex-to-base gradient in density of efferent terminals on OHCs (Maison et al., 2003a).

The magnitude of efferent effects was assessed in five mutant lines at 6 weeks of age. Efferent effects were normal in magnitude in four of the receptor-null lines, including all three of the normal-threshold lines, i.e., $\alpha 1$, $\alpha 2$, and δ (supplemental Fig. 3, available at www.jneurosci.org as supplemental material), and one line with modest threshold elevation at 6 weeks, i.e., $\alpha 5$ (Fig.

3*A*). In contrast, efferent suppression was significantly reduced for β2 mutants, the other line with threshold elevation (Fig. 3*B*). This efferent-effect reduction was present at test frequencies at which efferent effects are normally largest: by two-way ANOVA restricted to 11–32 kHz, the β2 group yields $F_{(1,16)} = 8.180$ and $p < 0.011$.

Vulnerability to temporary acoustic injury

There is evidence that the cochlear efferent system can protect the ear from acoustic injury (Rajan, 1988, 1995; Kujawa and Liberman, 1997; Zheng et al., 1997a,b; Maison and Liberman, 2000; Maison et al., 2002), and one component of acute acoustic damage to the inner ear is a glutamate excitotoxicity in the terminals of cochlear afferents (Puel et al., 1998). There is also evidence, in cerebellar granule cells, that $GABA_A$ receptor antagonists protect cells from excitotoxicity (Babot et al., 2005). Thus, we tested whether the loss of $GABA_A$ receptor subunits altered the vulnerability of the ear to acute acoustic injury.

Age-matched wild-type and knock-out animals from the α5 and β2 lines were exposed for 2 h to a noise band (8–16 kHz) at 89 dB SPL. After a 12 h recovery period, noise-induced threshold shift were measured via ABRs (Fig. 4*A*,*C*) and DPOAEs (Fig. 4*B*,*D*). As is typical for this exposure in mice (Yoshida et al., 2000), threshold shifts were maximal near 16–22 kHz for both genotypes. Mean values of threshold shift were not significantly different between mutant and wild-type mice, for either gene deletion, when examined over the whole range of test frequencies: by two-way ANOVA, the α5 group ABR yielded $F_{(1,9)} = 0.030$ and $p > 0.05$, whereas DPOAE yielded $F_{(1,4)} = 2.682$ and $p > 0.05$; the β2 group ABR yielded $F_{(1,12)} = 2.075$ and $p > 0.05$, whereas DPOAE yielded $F_{(1,14)} = 0.764$ and $p > 0.05$.

At high frequencies, there is a tendency toward less threshold shift in the mutant line. Indeed, for some of the comparisons, genotypic differences (barely) achieve statistical significance if attention is restricted to the three highest test frequencies, e.g., for the β2 ABR data, two-way ANOVA restricted to 22–45 kHz yields $F_{(1,12)} = 5.477$ and $p = 0.037$. These differences must be viewed cautiously because the preexposure thresholds in the mutants are higher than wild type and because high preexposure thresholds restrict the magnitude of the shift that can be measured by either ABR or DPOAE tests.

A week after exposure, mean threshold shifts ranged from ~0–10 dB in both wild types and mutants, in both lines (data not shown), demonstrating the almost complete reversibility of the damage after this exposure. No significant differences were observed between wild types and mutants in the recovery from acoustic overexposure.

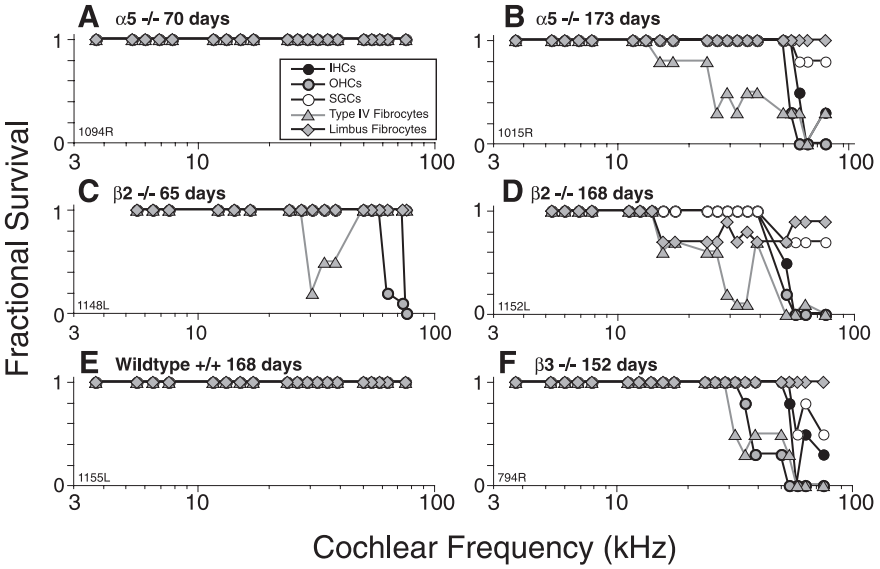

Figure 5. At 6–10 weeks, $GABA_A$ mutants show minimal cochlear histopathology at the light microscopic level; at >24 weeks, all three strains with threshold elevation show a similar pattern of basal-turn histopathology. Representative cases are illustrated here. Total numbers of cochleas evaluated can be extracted from Table 1. Details of techniques for relating cochlear positions in the sections to cochlear frequency are described in Materials and Methods.

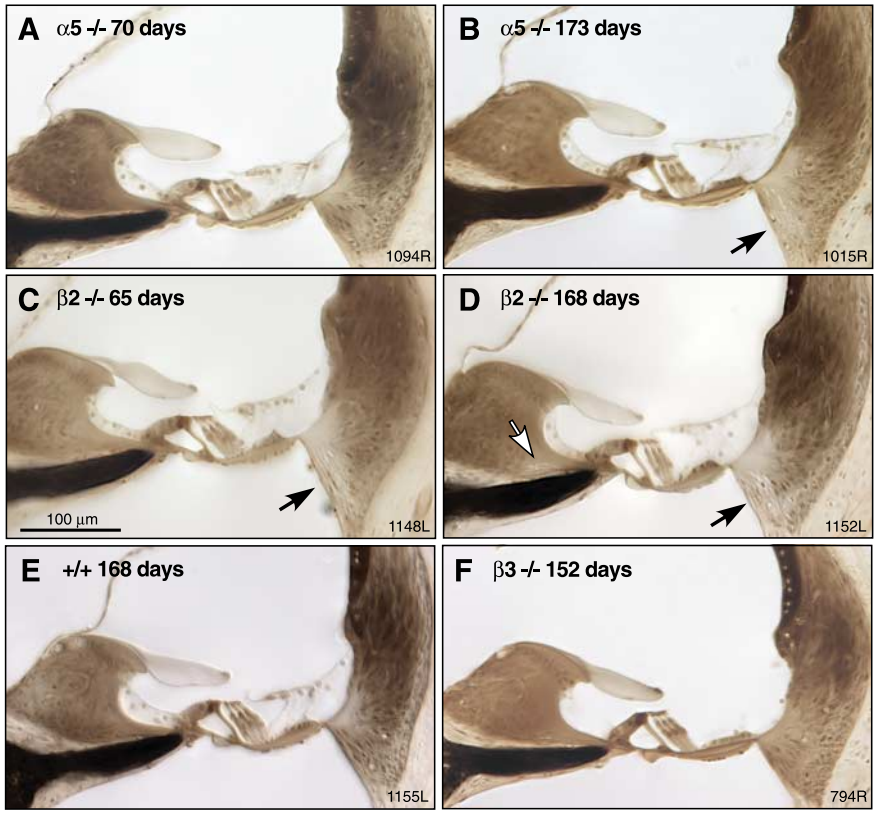

Figure 6. Photomicrographs illustrating the cochlear histopathology seen in the $GABA_A$ mutant strains with cochlear threshold elevations. The six cases illustrated here show the 30 kHz location from each of the same six cases for which the quantitative analyses are shown in Figure 5. Filled arrows in ***B–D*** point to the spiral ligament in which there is degeneration of type IV fibrocytes. The open arrow in ***D*** points to a small region of fibrocyte loss in the limbus near the osseous spiral lamina. The numbers above each panel give the age at which each animal was killed. Scale bar in ***C*** applies to all images.

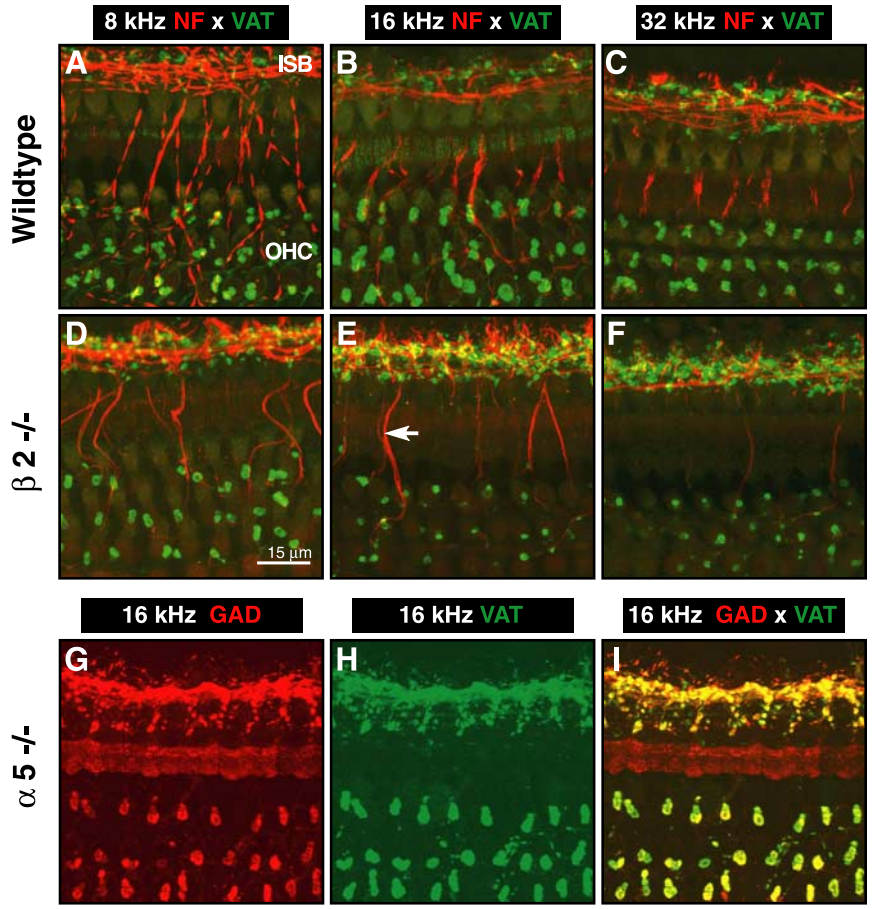

Figure 7. Immunostaining for a cholinergic marker (VAT) and a GABAergic marker (GAD) reveals loss of OHC efferent terminals in the β2 null at 6 weeks (***D–F***) but not the α5 null (***G–I***) compared with age-matched controls (***A–C***). ***A–F*** show projections from confocal *z*-stacks through cochlear whole mounts double stained for VAT (green) and NF-200 (red). Only merged images are shown. In *x* and *y*, the images span the organ of Corti from the OHCs to the inner spiral bundle (ISB). In *z*, the stack spans the region in which efferent terminals are found. Three cochlear regions are shown: 8 kHz (***A***, ***D***), 16 kHz (***B***, ***E***), and 32 kHz (***C***, ***F***). ***G–I***, Double staining for VAT (green, ***H***) and GAD (red, ***G***) shows normal efferent innervation in the 16 kHz region of an α5 null ear and the normal pattern of colocalization of GABAergic and cholinergic markers. Scale bar in ***D*** applies to all panels.

Cochlear histopathology

At the light microscopic level, all structures of the cochlear duct were examined in serial plastic-embedded sections through the inner ear.

At 6 weeks, cochleas of mutants from the four lines without functional phenotype (α1, α2, α6, and δ) were indistinguishable from wild-type littermates (data not shown; numbers of ears evaluated are shown in Table 1). At 6–10 weeks, cochleas from α5 and β2 lines showed minimal hair cell loss outside of the extreme cochlear base (Figs. 5*A*,*C*, 6*A*,*C*) and no other histopathology besides loss of type IV fibrocytes in the spiral ligament of the basal turn (Figs. 5*C*, 6*C*). No animals from the rare β3 line were killed at 6 weeks.

At ~24 weeks, α5, β2, and β3 nulls all showed virtually complete loss of inner and outer hair cells throughout the basal 15% of the cochlear spiral (Fig. 5*B*,*D*,*F*), i.e., from ~40 to 90 kHz according to the cochlear frequency map for mouse (Muller et al., 2005). Although this spiral gradient of damage does not mirror the apex-to-base gradient of GABAergic innervation density (Maison et al., 2003a), the hair cells of the extreme base are particularly vulnerable to a range of cochlear manipulations (Wang et al., 2002), and there are previous reports suggesting that long-term effects of cochlear de-efferentation in the adult include hair cell loss in the basal turn (X. Y. Zheng et al., 1999).

In addition, there was partial loss of spiral ganglion cells but only in cochlear regions in which inner hair cells were destroyed. There was also widespread loss of type IV fibrocytes, seen in all ears and spreading farther apically than at the 6 week survival (Figs. 5*B*,*D*,*F*, 6*B*,*D*,*F*). In the β2 line only, there was also widespread loss of a small population of fibrocytes in the spiral limbus, always positioned near where the limbus meets the osseous spiral lamina (Figs. 5*D*, 6*D*). This characteristic pattern of limbic degeneration was seen in all β2 ears examined at >24 week survival. As can be seen in Figure 6, these fibrocyte losses, although clear-cut, represent only a small fraction of the cells in the spiral ligament and spiral limbus, which otherwise appear quite normal in the mutant lines. No changes in the stria vascularis were evident in this light microscopic evaluation.

Abnormalities in afferent and efferent innervation

Immunostaining of cochlear whole mounts revealed abnormalities in both the afferent and efferent innervation of the cochlea in the mutant lines. Anti-NF immunostaining reveals all of the unmyelinated fibers within the organ of Corti. Although it stains both afferent and efferent fiber populations, the characteristic spatial organization of these two fiber classes allows for them to be differentiated, at least in broad outline. In some ears, anti-neurofilament was combined with immunostaining for VAT, which, in mouse, stains all efferent terminals under the OHCs and in the inner spiral bundle, from which contacts with cochlear nerve fibers and inner hair cells arise (Maison et al., 2003a). In others, VAT staining was combined with staining for glutamic acid decarboxylase (GAD), to assess the extent of colocalization of cholinergic and GABAergic markers in the efferent terminals.

The efferent innervation of OHCs was dramatically and selectively reduced in all three mutant lines with threshold shift, although the age of onset of the reduction differed among the three. Loss of afferent fibers was seen only in the β3 mutants.

At 6 weeks, the β2 null ears already showed loss of efferent terminals: confocal images (Fig. 7*D–F*) of anti-VAT (green)-stained sensory cells shows reduced density of efferent terminals under OHCs in all cochlear regions compared with place-matched images from wild-type ears (Fig. 7*A–C*). The partial OHC de-efferentation is also seen in the reduced number of tunnel-crossing NF-stained (red) axons headed for the OHC region (Fig. 7*E*, arrow). This partial de-efferentation is consistent with the reduction in shock-evoked efferent effects in the β2 null ears tested at the same age (Fig. 3*B*).

At 6 weeks, the efferent innervation density in the α5 nulls was normal: compare VAT staining of efferent terminals in Figure 7, *H* and *B*. This is consistent with the normal magnitudes of shock-evoked efferent effects seen in these mutants when tested at the same age (Fig. 3*A*). Double staining for VAT and GAD in these ears shows

that the normal colocalization of GABAergic and cholinergic markers presynaptically has not been disturbed by the loss of the α5 receptor in these mutants (Fig. 7*G–I*).

To determine whether the reduced innervation in β2 mutants represents a failure of development or a postdevelopmental degeneration, we examined ears at 10 and 21 d. As shown in Figure 8, efferent terminals develop normally in both α5 and β2 mutants: innervation of the first row first appears at approximately postnatal day 10 (P10) (Fig. 8*C*,*E*) and is fully developed by P21 (Fig. 8*D*,*F*). By 24 weeks, degeneration of OHC efferent terminals was also seen in α5 mutants: VAT-positive terminals were reduced to a degree comparable with that seen in the β2 mutants at 6 weeks (data not shown).

In β3 mutants at 24 weeks (Fig. 9), anti-NF staining also revealed a decrease in OHC efferent innervation. Low-power views (Fig. 9*A*,*D*) show reduced number of tunnel-crossing efferent axons in the β3 mutant compared with the same cochlear region of the age-matched wild type. The high-power views (Fig. 9*B*,*C* vs *E*,*F*), acquired as a *z*-stack, also reveal a decrease in the afferent innervation of inner hair cells. To view these cochlear nerve afferent terminals, we crop the *z*-series over the inner spiral bundle (dashed rectangle in *B* and *E*) and rotate to view as an *x–z* projection (*C* and *F*). In this "side" view, afferent terminals are seen as thin stalks rising from the region of the inner spiral bundle and ending as terminal swellings (e.g., open arrowhead in *C*). Comparison of the stacks suggests a significant loss of afferent terminals in the null ear; similar findings were made in the only other β3 null ear immunostained for innervation analysis. Analysis of similar anti-NF-stained image stacks from β2 and α5 null and wild-type ears failed to reveal any significant loss of afferent terminals in these other two lines (data not shown).

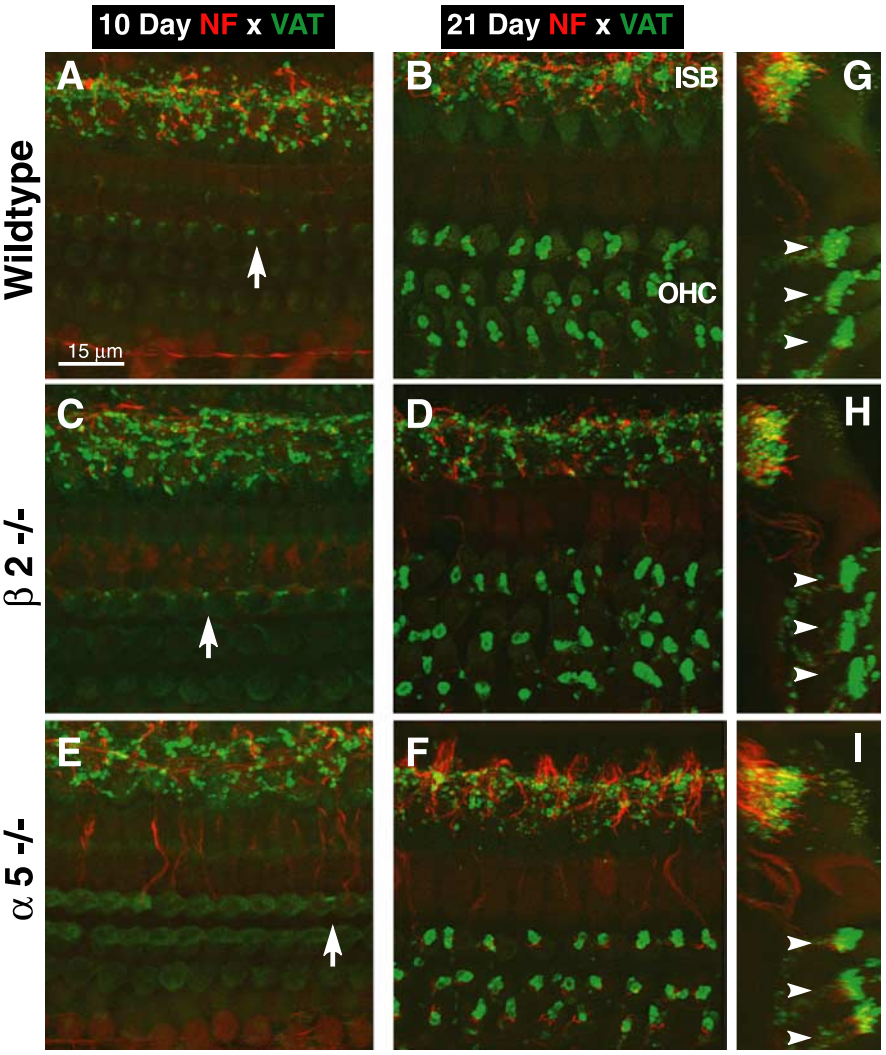

Figure 8. Immunostaining for VAT (green) and NF (red) in developing mice reveals a normal density of OHC efferent terminals at P10 and P21 in both β2 and α5 nulls. ***A–F***, *x–y* projections from confocal *z*-stacks through cochlear whole mounts from the 16 kHz region: only merged images are shown. In *x* and *y*, the images span the organ of Corti from the OHCs to the inner spiral bundle (ISB). In *z*, the stack spans the region in which efferent terminals are found. Arrows indicate nascent efferent terminals under first-row OHCs in the P10 images. ***G–I***, *y–z* projections of the 21 d images. Arrowheads point to the efferent terminal clusters under each of the three rows of OHCs. Scale bar in ***A*** applies to all panels.

The loss of efferent innervation seen in the three receptor mutants could reflect degeneration of the peripheral terminals arising from either loss of GABA signaling with OHCs or from loss of the neuron itself attributable to loss of somatic signaling from its GABAergic inputs. To distinguish these possibilities, we stained brainstems for acetylcholinesterase (AChE), which, in the vicinity of the olivary complex, labels only olivocochlear neurons (Campbell and Henson, 1988; Brown, 1993): Figure 10 shows a normal complement of AChE-positive olivocochlear neurons in the β2 mutant at 4 months, well beyond the age at which the cochlear efferent terminals have disappeared.

Localization of receptor subunits

Localization of $GABA_A$ receptor subunits was studied immunohistochemically for α5, β2, and β3, the three subunits for which deletion led to a cochlear phenotype. For all antibodies used, the null mice for the receptor in question were used as negative controls to ensure the specificity of the resultant label. Only material from 6 week animals was examined.

For β2 and β3 subunits, there was diffuse immunostaining in OHCs especially in the apical half of the cochlea (Fig. 11*A*). Using an antibody that cross-reacts with both β2 and β3 subunits, we also saw staining in the inner spiral bundle area beneath the inner hair cells (Fig. 11*B*). With an antibody specific for the β3 subunit, we saw punctate staining ringing the cell bodies of selected spiral ganglion cells and the axoplasm of selected neuronal processes in the osseous spiral lamina (Fig. 11*C*,*D*). For the α5 subunit, we were unable to produce any reliable immunostaining in the wild-type that was absent in the null.

No attempts were made to immunostain cochleas for α1, α2, or δ subunits, which produced no cochlear phenotype when deleted. However, the α6 null line was created with a lacZ reporter gene insert that may be useful in assessing the expression pattern: when reacted appropriately, cochlear sections from the homozygous null animals showed no signal; cerebellar granule cells from the same animals served as a positive control.

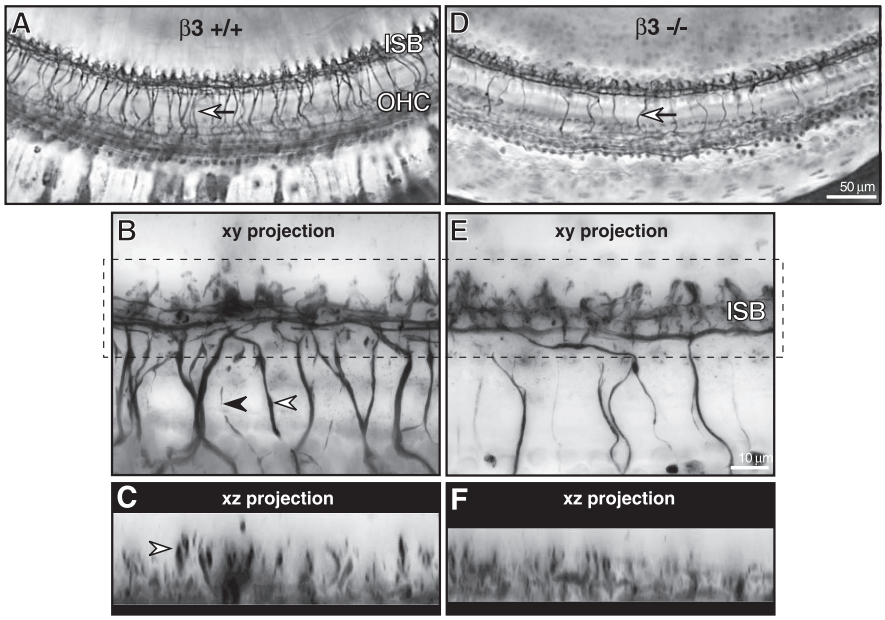

Figure 9. Anti-neurofilament immunostaining reveals a reduction in afferent and efferent innervation of hair cells in the $GABA_A$ β3 nulls at 24 weeks. ***A*** and ***D*** show low-power views from the middle of the cochlea in a wild type and β3 null, respectively. The image is focused at the level of the tunnel of Corti at which efferent axons (open arrows) cross to OHCs. The inner spiral bundle (ISB) contains spiraling efferents in the region under IHCs. Scale bar in ***D*** applies to ***A*** as well. ***B*** and ***E*** show high-power (100× objective) *z*-series projections from selected regions of the same cochlear pieces shown in ***A*** and ***D***, respectively. These images constitute the superposition (darkest pixel) of 75 images acquired at 0.5 μm intervals, spanning the focal depths over which fibers cross from the inner spiral bundle to the OHCs, including both thin OHC afferents (filled arrowhead) and thicker OHC efferents (open arrowhead). ***C*** and ***F*** show the *x–z* projections of the same image stacks shown in ***B*** and ***E***, respectively, first cropped to include only the IHC region (see dashed lines in ***B*** and ***E***). This projection reveals immunostained afferent terminals (e.g., open arrowhead in ***C***) contacting the sides of IHCs. Scale bar in ***E*** applies to ***B***, ***C***, and ***F*** as well.

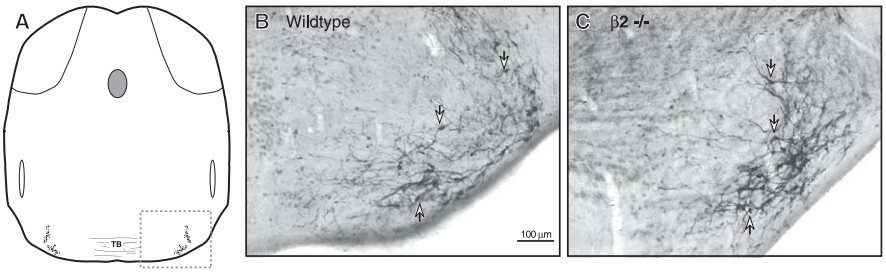

Figure 10. AChE staining shows medial olivocochlear neurons and their proximal dendrites in the superior olivary complex: even at 4 months of age, there is no obvious loss of olivocochlear neurons in the β2 null mutants. Photomicrographs in ***B*** and ***C*** are taken from the ventral regions of the olivary complex (schematic in ***A***), just rostral to the rostral tip of the lateral superior olivary nuclei, in which the concentration of medial olivocochlear neurons is greatest. Arrows point to AChE-positive cell bodies in each image.

Discussion

Cochlear GABAergic innervation and receptor subunit expression

There is a robust GABAergic efferent innervation in developing and adult cochleas. In mouse and rat, GABAergic efferent terminals appear in the IHC area by P0 and on OHCs by P7 (Whitlon and Sobkowicz, 1989). In the developing IHC area, these terminals contact both IHCs and afferent terminals. In the adult, GABAergic innervation of the IHC area extends throughout the cochlea, whereas the extent of GABAergic OHC innervation varies with species: in guinea pig, it is restricted to the apical half of the cochlea (Eybalin, 1993), whereas in mouse, it is present from base to apex, and GABAergic and cholinergic markers colocalize in efferent terminals in both IHC and OHC areas (Maison et al., 2003a).

An RT-PCR study reports that the mouse inner ear, at P14–P18, contains all three β subunits, all six α subunits, and the γ2 subunit (not γ1 or γ3) but does not contain the δ subunit (Drescher et al., 1993). Studies in rat confirm the presence of α1–α6, β1–β3, and γ1–γ3 and the absence of δ in the vestibular portion of the inner ear (Cheng and Kong, 2003). Immunohistochemical and *in situ* hybridization studies confirm the patterns reported here, i.e., that α and β subunits, including α1, α2, α5, β2, and β3, are expressed in tissues targeted by GABAergic efferents, i.e., OHCs and spiral ganglion cells, or the neuropil under IHCs (Zheng et al., 2004).

Based on these data, the lack of cochlear phenotype in the δ knock-out may reflect a lack of cochlear expression. The lack of cochlear phenotype for α1, α2, and α6 is more surprising, because α2 and α6 are reportedly plentiful in the cochlea (Drescher et al., 1993). Compensatory changes in other α subunits [e.g., α2 and α3 are upregulated in α1 knock-outs (Kralic et al., 2002)] may mask a cochlear phenotype. Alternatively, the relevant GABAergic system for the receptors containing these subunits may not be "engaged" by our assays. However, our ABR/DPOAE assay has detected subtle changes in neurotransmission by IHC area efferents, e.g., in mice lacking calcitonin gene-related peptide, a transmitter colocalized with GABA and ACh (Maison et al., 2003b).

The cochlear phenotypes seen with loss of α5, β2, or β3 suggest that these subunits are important in the mature ear (see below). Given that β3 does not substitute for β2 and vice versa (Rudolph and Mohler, 2004) and the cochlear subunit distribution summarized above, it appears that GABAergic targets in the cochlea express at least α5β2γ and α5β3γ receptor complexes. However, the phenotypic differences between α5 and β2 nulls (i.e., only β2 null showed sex differences and a neural component to the progressive threshold shifts) suggest that other receptor combinations also participate.

Minimal GABAergic effects on signal processing

GABA effects on OHCs and the cochlear amplifier

OHCs display electromotility (Brownell, 1990) that drives a cochlear amplification process that mediates threshold sensitivity (Liberman et al., 2002). GABA application on guinea pig OHCs can reduce electromotility, hyperpolarize the cells, and alter their stiffness (Sziklai et al., 1996; Batta et al., 2004). When present, these effects are (1) blocked by picrotoxin and potentiated by benzodiazepines (Gitter and Zenner, 1992), consistent with $GABA_A$ receptors, including a γ subunit, and (2) restricted to apical OHCs, consistent with evidence that GABAergic terminals in guinea pigs are restricted to apical OHCs (Fex and Altschuler, 1986).

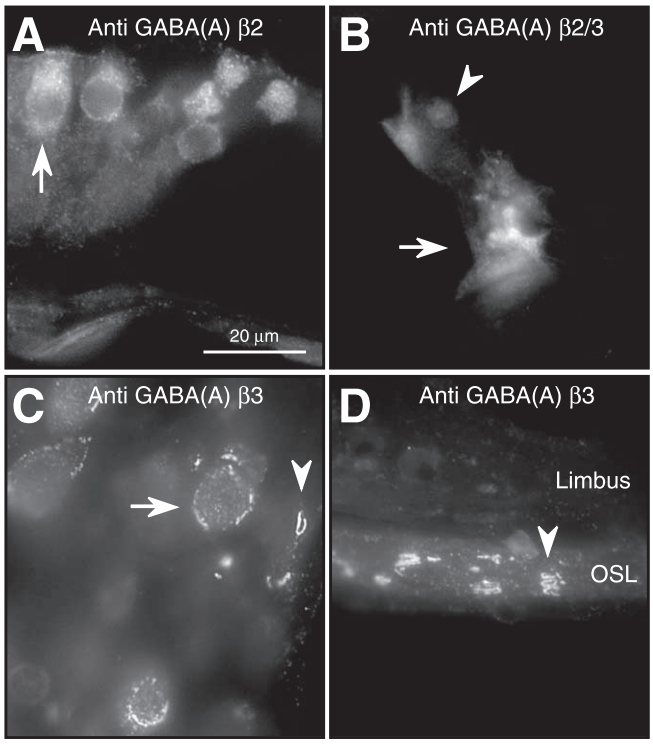

Figure 11. Immunostaining patterns in wild-type ears for $GABA_A$ $\beta 2$ and $\beta 3$ subunits. ***A***, Outer hair cells stained with an antibody to the $GABA_A$ $\beta 2$ subunit. An OHC from the third row is shown at the arrow. ***B***, Fibers and terminals in the inner spiral bundle area (white arrow) immunostained with an antibody to both $\beta 2$ and $\beta 3$ subunits. The arrowhead points to the IHC nucleus. ***C***, Immunolabeling of the perimeter of selected spiral ganglion cells (white arrow) and selected axons (arrowhead) with an antibody to the $GABA_A$ $\beta 3$ subunit. ***D***, Immunolabeling outlines selected peripheral axons in the osseous spiral lamina (OSL) using the same anti-$\beta 3$ antibody as in ***C***. Scale bar in ***A*** applies to all images.

Thus, GABA release from OHC efferent terminals *in vivo* might elevate cochlear thresholds. Indeed, OHC efferents comprise the effector arm of a negative-feedback loop, which reduces OHC contributions to cochlear amplification and raises cochlear thresholds, as seen in our assays (Fig. 3). However, this efferent-mediated suppression disappears in a mouse lacking the $\alpha 9$ nicotinic ACh receptor (Vetter et al., 1999), despite the maintenance of a robust OHC efferent innervation. Given that GABA and ACh are colocalized in OHC efferents and assuming that GABA is released from efferent terminals, such negative results are not consistent with an independent effect of GABA on OHC electromotility *in vivo*.

In humans, benzodiazepines decrease the magnitude of efferent-mediated suppression of otoacoustic emissions elicited by contralateral sound (Morand et al., 1998). Although this effect could arise in the cochlea, an enhancement of GABAergic effects at this locus should enhance cochlear suppression rather than reduce it. Furthermore, the central circuitry driving this sound-evoked reflex likely includes GABAergic inhibitory inputs, whose actions could be enhanced by benzodiazepines, thus producing the observed reduction in reflex strength.

Rather than subserving an independent action on OHC motility, GABA at the OHC/efferent synapse could modulate cholinergic effects. Indeed, we found reduction in electrically evoked efferent suppression in $\beta 2$ nulls (Fig. 3). However, histological analysis revealed a reduction in density of OHC efferents. Thus, our data suggest a GABAergic role in maintenance of the efferent innervation rather than in the phasic modulation of their peripheral effects.

GABA effects on IHCs and sensory neurons

There are few studies of GABAergic effects on IHCs or primary sensory neurons. One *in vitro* study on neonatal spiral ganglion cells reports that GABA elicits inward currents with $GABA_A$ pharmacology (Malgrange et al., 1997), whereas another reports $GABA_B$-like effects (Lin et al., 2000). In the lateral line, GABA depresses spontaneous neural discharge, but the pharmacology and the site of action have not been extensively investigated (Bobbin et al., 1985; Mroz and Sewell, 1989). *In vivo* data for the mammalian ear are limited to cochlear perfusion in guinea pig in which GABA decreased glutamate-induced spiking in apical afferents without affecting background spontaneous rates (Felix and Ehrneberger, 1992).

Unmyelinated efferents innervating cochlear afferents and IHCs are not activated by shocks at the site used in this study (Guinan, 1996). However, indirect activation by shocking the inferior colliculus causes slow changes in cochlear nerve response, either excitation or inhibition depending on the locus stimulated, suggesting that two complementary feedback systems titrate the excitability of cochlear nerve dendrites (Groff and Liberman, 2003). A GABAergic subsystem is an obvious candidate for the inhibitory pathway; however, present results do not support this idea. Loss of four of the $GABA_A$ receptor subunits had no effect on cochlear nerve thresholds or evoked neural amplitudes. The phenotypes observed in the other three ($\alpha 5$, $\beta 2$, and $\beta 3$) include clear evidence for cochlear nerve abnormalities (loss of afferent terminals in the $\beta 3$ and disproportionate elevation of ABR thresholds in the $\beta 2$), but the nature of the changes, and their progression with age, suggest a role for GABA in the maintenance of afferent innervation rather than in phasic modulation of its excitability.

Dramatic GABAergic effects on neuronal maintenance and sexual dimorphism

In mice and humans, there are gender differences in cochlear function and dysfunction, e.g., in age-related hearing loss (Henry, 2002). The gender effect in the $\beta 2$ cochlear phenotype is interesting, because GABA has been implicated in sexual differentiation of the brain via estradiol-induced differences in chloride concentration in target cells, which influence the timing of the developmental transition from excitatory to inhibitory GABAergic effects (McCarthy et al., 2002). Both rat and mouse inner ear express estrogen receptors, especially on type I ganglion cells (Stenberg et al., 1999), the generators of the neural responses severely affected in the $\beta 2$ nulls.

The phenotypes observed in all affected $GABA_A$ knock-out lines suggest OHC dysfunction (DPOAE threshold elevation), dysfunction of primary sensory neurons (ABR elevation $>$ DPOAE elevations), and partial de-efferentation of OHCs. In addition, the $\beta 3$ line showed partial de-afferentation of IHCs (Fig. 9), as well as shrinkage of calretinin-positive spiral ganglion cells (Koo et al., 2002). The observation that threshold elevations are progressive (in both $\alpha 5$ and $\beta 2$; $\beta 3$ not tested) indicate that the GABAergic innervation of the cochlea is important in maintenance of both hair cells and neurons. The mechanisms are unclear, but GABAergic transmission in the CNS can decrease glutamatergic activity (Green et al., 2000), and glutamate-induced excitotoxicity causes acute damage to cochlear nerve terminals (Puel et al., 1998) and may initiate slow-onset neuronal degeneration seen in mice aging after early noise exposure (Kujawa and

Liberman, 2006). Adult-onset degeneration of cochlear neurons is also seen with targeted deletion of the β2 nicotinic ACh receptor (Bao et al., 2005).

The observation that the efferent innervation of OHCs develops normally in α5 and β2 nulls and then degenerates, rapidly in the β2 (by 6 weeks) and less rapidly in the α5 (by 24 weeks), demonstrates a key role for GABAergic transmission in long-term maintenance of efferent synaptic terminals The observation that somata of OHC efferents in the superior olive are normal in number and dendritic morphology several months after their peripheral terminals have disappeared implies that the neuronal degeneration in the cochlea does not arise from the loss of GABAergic synaptic transmission between the olivocochlear neuron and its central circuitry; rather, it arises because of the loss of GABAergic signaling between the OHC and its efferent synapse.

In summary, our results suggest minimal short-term influence of $GABA_A$ signaling on cochlear responses to sound but important long-term influences on health of sensory cells and their innervation. The progressive nature of the degenerative changes seen after perturbation of GABAergic signaling suggests a role for GABA in the etiology of sensorineural hearing loss in general and age-related hearing loss in particular.

References

Arnold T, Oestreicher E, Ehrenberger K, Felix D (1998) GABA(A) receptor modulates the activity of inner hair cell afferents in guinea pig cochlea. Hear Res 125:147–153.

Bao J, Lei D, Du Y, Ohlemiller KK, Beaudet AL, Role LW (2005) Requirement of nicotinic acetylcholine receptor subunit β2 in the maintenance of spiral ganglion neurons during aging. J Neurosci 25:3041–3045.

Babot Z, Cristofol R, Sunol C (2005) Excitotoxic death induced by released glutamate in depolarized primary cultures of mouse cerebellar granule cells is dependent on GABAA receptors and niflumic acid-sensitive chloride channels. Eur J Neurosci 21:103–112.

Batta TJ, Panyi G, Szucs A, Sziklai I (2004) Regulation of the lateral wall stiffness by acetylcholine and GABA in the outer hair cells of the guinea pig. Eur J Neurosci 20:3364–3370.

Bobbin RP, Bledsoe Jr SC, Winbery S, Ceasar G, Jenison GL (1985) Comparative actions of GABA and acetylcholine on the *Xenopus laevis* lateral line. Comp Biochem Physiol C 80:313–318.

Boehm II SL, Ponomarev I, Jennings AW, Whiting PJ, Rosahl TW, Garrett EM, Bledsoe YA, Harris RA (2004) γ-Aminobutyric acid A receptor subunit mutant mice: new perspectives on alcohol actions. Biochem Pharmacol 68:1581–1602.

Brown MC (1993) Fiber pathways and branching patterns of biocytin-labeled olivocochlear neurons in the mouse brainstem. J Comp Neurol 337:600–613.

Brownell WE (1990) Outer hair cell electromotility and otoacoustic emissions. Ear Hear 11:82–92.

Campbell JP, Henson MM (1988) Olivocochlear neurons in the brainstem of the mouse. Hear Res 35:271–274.

Cheng H, Kong W (2003) Expression of gamma-aminobutyric acid receptor gamma 1 subunit in the end-organs of rat vestibule. Lin Chuang Er Bi Yan Hou Ke Za Zhi 17:229–230.

Collinson N, Kuenzi FM, Jarolimek W, Maubach KA, Cothliff R, Sur C, Smith A, Otu FM, Howell O, Atack JR, McKernan RM, Seabrook GR, Dawson GR, Whiting PJ, Rosahl TW (2002) Enhanced learning and memory and altered GABAergic synaptic transmission in mice lacking the α5 subunit of the $GABA_A$ receptor. J Neurosci 22:5572–5580.

DeLorey TM, Handforth A, Anagnostaras SG, Homanics GE, Minassian BA, Asatourian A, Fanselow MS, Delgado-Escueta A, Ellison GD, Olsen RW (1998) Mice lacking the beta3 subunit of the $GABA_A$ receptor have the epilepsy phenotype and many of the behavioral characteristics of Angelman syndrome. J Neurosci 18:8505–8514.

Drescher DG, Green GE, Khan KM, Hajela K, Beisel KW, Morley BJ, Gupta AK (1993) Analysis of gamma-aminobutyric acidA receptor subunits in the mouse cochlea by means of the polymerase chain reaction. J Neurochem 61:1167–1170.

Dulon D, Zajic G, Schacht J (1990) Increasing intracellular free calcium induces circumferential contractions in isolated cochlear outer hair cells. J Neurosci 10:1388–1397.

Evans MG, Kiln J, Pinch D (1996) No evidence for functional GABA receptors in outer hair cells isolated from the apical half of the guinea-pig cochlea. Hear Res 101:1–6.

Eybalin M (1993) Neurotransmitters and neuromodulators of the mammalian cochlea. Physiol Rev 73:309–373.

Felix D, Ehrenberger K (1992) The efferent modulation of mammalian inner hair cell afferents. Hear Res 64:1–5.

Fex J, Altschuler RA (1986) Neurotransmitter-related immunochemistry of the organ of Corti. Hear Res 22:249–263.

Gitter AH, Zenner HP (1992) γ-Aminobutyric acid receptor activation of outer hair cells in the guinea pig cochlea. Eur Arch Otorhinolaryngol 249:62–65.

Green AR, Hainsworth AH, Jackson DM (2000) GABA potentiation: a logical pharmacological approach for the treatment of acute ischaemic stroke. Neuropharmacology 39:1483–1494.

Groff JA, Liberman MC (2003) Modulation of cochlear afferent response by the lateral olivocochlear system: activation via electrical stimulation of the inferior colliculus. J Neurophysiol 90:3178–3200.

Guinan Jr JJ (1996) The physiology of olivocochlear efferents. In: The cochlea (Dallos PJ, Popper AN, Fay RR, eds), pp 435–491. New York: Springer.

Guinan JJ, Gifford ML (1988) Effects of electrical stimulation of efferent olivocochlear neurons on cat auditory-nerve fibers. III. Tuning curves and thresholds at CF. Hear Res 37:29–46.

Henry KR (2002) Sex- and age-related elevation of cochlear nerve envelope response (CNER) and auditory brainstem response (ABR) thresholds in C57BL/6 mice. Hear Res 170:107–115.

Homanics GE, DeLorey TM, Firestone LL, Quinlan JJ, Handforth A, Harrison NL, Krasowski MD, Rick CE, Korpi ER, Makela R, Brilliant MH, Hagiwara N, Ferguson C, Snyder K, Olsen RW (1997) Mice devoid of gamma-aminobutyrate type A receptor β3 subunit have epilepsy, cleft palate, and hypersensitive behavior. Proc Natl Acad Sci USA 94:4143–4148.

Jimenez AM, Stagner BB, Martin GK, Lonsbury-Martin BL (1999) Age-related loss of distortion product otoacoustic emissions in four mouse strains. Hear Res 138:91–105.

Jones A, Korpi ER, McKernan RM, Pelz R, Nusser Z, Makela R, Mellor JR, Pollard S, Bahn S, Stephenson FA, Randall AD, Sieghart W, Somogyi P, Smith AJ, Wisden W (1997) Ligand-gated ion channel subunit partnerships: $GABA_A$ receptor α6 subunit gene inactivation inhibits δ subunit expression. J Neurosci 17:1350–1362.

Kempf HG, Brandle TU, Wisden W, Zenner HP (1994) γ-Aminobutyric acidA-receptor messenger ribonucleic acid (α-1 subunit) detection by in situ hybridization. Eur Arch Otorhinolaryngol 251:61–64.

Kempf HG, Brandle TU, Wisden W, Zenner HP, Marx A (1995) Detection of $GABA_A$ receptor mRNA in cochlear tissue. An in situ hybridization study (in German). HNO 43:12–18.

Kirk DL, Johnstone BM (1993) Modulation of f2–f1: evidence for a GABAergic efferent system in apical cochlea of the guinea pig. Hear Res 67:20–34.

Koo JW, Homanics GE, Balaban CD (2002) Hypoplasia of spiral and Scarpa's ganglion cells in $GABA_A$ receptor beta(3) subunit knockout mice. Hear Res 167:71–80.

Kralic JE, Korpi ER, O'Buckley TK, Homanics GE, Morrow AL (2002) Molecular and pharmacological characterization of $GABA_A$ receptor alpha1 subunit knockout mice. J Pharmacol Exp Ther 302:1037–1045.

Kujawa SG, Liberman MC (1997) Conditioning-related protection from acoustic injury: effects of chronic deefferentation and sham surgery. J Neurophysiol 78:3095–3106.

Kujawa SG, Liberman MC (2006) Acceleration of age-related hearing loss by early noise exposure: evidence of a misspent youth. J Neurosci 26:2115–2123.

Kujawa SG, Fallon M, Bobbin RP (1995) Time-varying alterations in the f2–f1 DPOAE response to continuous primary stimulation. I. Response characterization and contribution of the olivocochlear efferents. Hear Res 85:142–154.

Liberman MC, Gao WY (1995) Chronic cochlear de-efferentation and susceptibility to permanent acoustic injury. Hear Res 90:158–168.

Liberman MC, Chesney CP, Kujawa SG (1997) Effects of selective inner hair

cell loss on DPOAE and CAP in carboplatin-treated chinchillas. Aud Neurosci 3:255–268.
Liberman MC, Gao J, He DZ, Wu X, Jia S, Zuo J (2002) Prestin is required for electromotility of the outer hair cell and for the cochlear amplifier. Nature 419:300–304.
Lin X, Chen S, Chen P (2000) Activation of metabotropic GABAB receptors inhibited glutamate responses in spiral ganglion neurons of mice. NeuroReport 11:957–961.
Lukashkin AN, Lukashkina VA, Russell IJ (2002) One source for distortion product otoacoustic emissions generated by low- and high-level primaries. J Acoust Soc Am 111:2740–2748.
Maison SF, Liberman MC (2000) Predicting vulnerability to acoustic injury with a noninvasive assay of olivocochlear reflex strength. J Neurosci 20:4701–4707.
Maison SF, Liberman MC (2006) Characterization of electrically evoked olivocochlear fast and slow effects in mice. ARO Abstr:881.
Maison SF, Luebke AE, Liberman MC, Zuo J (2002) Efferent protection from acoustic injury is mediated via α9 nicotinic acetylcholine receptors on outer hair cells. J Neurosci 22:10838–10846.
Maison SF, Adams JC, Liberman MC (2003a) Olivocochlear innervation in the mouse: immunocytochemical maps, crossed versus uncrossed contributions, and transmitter colocalization. J Comp Neurol 455:406–416.
Maison SF, Emeson RB, Adams JC, Luebke AE, Liberman MC (2003b) Loss of alpha CGRP reduces sound-evoked activity in the cochlear nerve. J Neurophysiol 90:2941–2949.
Malgrange B, Rigo JM, Lefebvre PP, Coucke P, Goffin F, Xhauflaire G, Belachew S, Van der Water TR, Moonen G (1997) Diazepam-insensitive GABA A receptors on postnatal spiral ganglion neurons in culture. NeuroReport 8:591–596.
McCarthy MM, Auger AP, Perrot-Sinal TS (2002) Getting excited about GABA and sex differences in the brain. Trends Neurosci 25:307–312.
Melcher JR, Guinan Jr JJ, Knudson IM, Kiang NY (1996) Generators of the brainstem auditory evoked potential in cat. II. Correlating lesion sites with waveform changes. Hear Res 93:28–51.
Mihalek RM, Banerjee PK, Korpi ER, Quinlan JJ, Firestone LL, Mi ZP, Lagenaur C, Tretter V, Sieghart W, Anagnostaras SG, Sage JR, Fanselow MS, Guidotti A, Spigelman I, Li Z, DeLorey TM, Olsen RW, Homanics GE (1999) Attenuated sensitivity to neuroactive steroids in gamma-aminobutyrate type A receptor delta subunit knockout mice. Proc Natl Acad Sci USA 96:12905–12910.
Morand N, Veuillet E, Gagnieu MC, Lemoine P, Collet L (1998) Benzodiazepines alter cochleo-cochlear loop in humans. Hear Res 121:71–76.
Mroz EA, Sewell WF (1989) Pharmacological alterations of the activity of afferent fibers innervating hair cells. Hear Res 38:141–162.
Muller M, von Hunerbein K, Hoidis S, Smolders JW (2005) A physiological place-frequency map of the cochlea in the CBA/J mouse. Hear Res 202:63–73.
Osen KK, Roth K (1969) Histochemical localization of cholinesterases in the cochlear nuclei of the cat with notes on the origin of acetylcholinesterase-positive afferents and the superior olive. Brain Res 16:165–185.
Plinkert PK, Mohler H, Zenner HP (1989) A subpopulation of outer hair cells possessing GABA receptors with tonotopic organization. Arch Otorhinolaryngol 246:417–422.
Plinkert PK, Gitter AH, Mohler H, Zenner HP (1993) Structure, pharmacology and function of $GABA_A$ receptors in cochlear outer hair cells. Eur Arch Otorhinolaryngol 250:351–357.
Puel JL, Ruel J, Gervais d'Aldin C, Pujol R (1998) Excitotoxicity and repair of cochlear synapses after noise-trauma induced hearing loss. NeuroReport 9:2109–2114.
Rajan R (1988) Effect of electrical stimulation of the crossed olivocochlear bundle on temporary threshold shifts in auditory sensitivity. II. Dependence on the level of temporary threshold shifts. J Neurophysiol 60:569–579.
Rajan R (1995) Involvement of cochlear efferent pathways in protective effects elicited with binaural loud sound exposure in cats. J Neurophysiol 74:582–597.
Rudolph U, Mohler H (2004) Analysis of GABAA receptor function and dissection of the pharmacology of benzodiazepines and general anesthetics through mouse genetics. Annu Rev Pharmacol Toxicol 44:475–498.
Stenberg AE, Wang H, Sahlin L, Hultcrantz M (1999) Mapping of estrogen receptors alpha and beta in the inner ear of mouse and rat. Hear Res 136:29–34.
Sur C, Wafford KA, Reynolds DS, Hadingham KL, Bromidge F, Macaulay A, Collinson N, O'Meara G, Howell O, Newman R, Myers J, Atack JR, Dawson GR, McKernan RM, Whiting PJ, Rosahl TW (2001) Loss of the major $GABA_A$ receptor subtype in the brain is not lethal in mice. J Neurosci 21:3409–3418.
Sziklai I, He DZZ, Dallos P (1996) Effect of acetylcholine and GABA on the transfer function of electromotility in isolated outer hair cells. Hear Res 95:87–99.
Vetter DE, Liberman MC, Mann J, Barhanin J, Boulter J, Brown MC, Saffiote-Kolman J, Heinemann SF, Elgoyhen AB (1999) Role of alpha9 nicotinic ACh receptor subunits in the development and function of cochlear efferent innervation. Neuron 23:93–103.
Vicini S, Ortinski P (2004) Genetic manipulations of GABAA receptor in mice make inhibition exciting. Pharmacol Ther 103:109–120.
Vicini S, Ferguson C, Prybylowski K, Kralic J, Morrow AL, Homanics GE (2001) $GABA_A$ receptor alpha1 subunit deletion prevents developmental changes of inhibitory synaptic currents in cerebellar neurons. J Neurosci 21:3009–3016.
Wang Y, Hirose K, Liberman MC (2002) Dynamics of noise-induced cellular injury and repair in the mouse cochlea. J Assoc Res Otolaryngol 3:248–268.
Warr BW, Guinan Jr JJ (1979) Efferent innervation of the organ of Corti: two separate systems. Brain Res 173:152–155.
Whiting PJ (1999) The GABAA receptor gene family: new targets for therapeutic intervention. Neurochem Int 34:387–390.
Whitlon DS, Sobkowicz HM (1989) GABA-like immunoreactivity in the cochlea of the developing mouse. J Neurocytol 18:505–518.
Yamamoto Y, Matsubara A, Ishii K, Makinae K, Sasaki A, Shinkawa H (2002) Localization of gamma-aminobutyric acid A receptor subunits in the rat spiral ganglion and organ of Corti. Acta Otolaryngol 122:709–714.
Yoshida N, Hequembourg SJ, Atencio CA, Rosowski JJ, Liberman MC (2000) Acoustic injury in mice: 129/SvEv is exceptionally resistant to noise-induced hearing loss. Hear Res 141:97–106.
Zheng H, Tang YD, Zheng Y, Yang H (2004) Detection of GABAA alpha 2 mRNA in rat cochlear spiral neuron with in situ hybridization. Sichuan Da Xue Xue Bao Yi Xue Ban 35:182–184.
Zheng QY, Johnson KR, Erway LC (1999) Assessment of hearing in 80 inbred strains of mice by ABR threshold analyses. Hear Res 130:94–107.
Zheng XY, Henderson D, Hu BH, Ding DL, McFadden SL (1997a) The influence of the cochlear efferent system on chronic acoustic trauma. Hear Res 107:147–159.
Zheng XY, Henderson D, McFadden SL, Hu BH (1997b) The role of the cochlear efferent system in acquired resistance to noise-induced hearing loss. Hear Res 104:191–203.
Zheng XY, Henderson D, McFadden SL, Ding DL, Salvi RJ (1999) Auditory nerve fiber responses following chronic cochlear de-efferentation. J Comp Neurol 406:72–86.